

MEASUREMENT OF TRANSVERSE AND LONGITUDINAL SPECTRA

Mario Serio, Mikhail Zobov*

INFN - LNF - C.P. 13 , 00044 Frascati (Roma) - Italy

* On leave from M.E.P.I., Moscow 115409 - Russia

ABSTRACT

In this paper we discuss transverse and longitudinal spectra in circular accelerators and various measurement techniques.

INTRODUCTION

Apart from the association to ghosts and phantoms, the words *spectrum*, *spectral* also refer, in the common usage, to the rainbow-colored band into which a beam of sun light is decomposed by passing through a prism. In fact, in scientific jargon the word spectrum is used to indicate the distribution of the intensity of radiation as a function of energy, or the distribution of the amplitude (and phase) or energy of a wave as a function of frequency.

This latter acceptance is implied in the discussion which follows, with application to signals from pick-up's sensitive to the beam motion in a particle accelerator, with more emphasis in the observation techniques, rather than in the causes. The subject is broad and there are many practical and substantial differences between various accelerators, related to the size, intensity and type of particles accelerated and user requirements. Therefore, we illustrate a few general concepts and cite the references whereby separate topics have been treated for the first time, or more extensively.

Single particle and beam spectra in the presence of synchrotron and betatron oscillations are reviewed in Section 1. The Schottky noise (incoherent) and the concept of coherent modes of oscillation is also introduced.

In Section 2 we give a schematic classification of various types of longitudinal and transverse beam monitors and kickers.

Finally, in Section 3 we give an overview of the instrumentation and data analysis techniques involving measurements of the beam response to longitudinal and transverse excitation and their various uses.

Throughout the text the symbols ω and Ω denote *angular* frequency [$rad \cdot sec^{-1}$], while the symbol f denotes frequency [sec^{-1}].

1.- BEAM SPECTRA

The material presented in this section is mostly drawn from the treatment made by R. Littauer in [1], J. L. Laclare in [2], D. Boussard in [3].

1.1 Single Particle

1.1.1 Longitudinal

A single particle of charge e rotating with speed v in the central orbit of an accelerator of average radius of curvature R can be described by a time-dependent *linear charge density*

$$\lambda(t) = \frac{e}{v} \sum_{k=-\infty}^{\infty} \delta(t - kT_0), \quad (1.1)$$

where T_0 is the revolution time $T_0 = 2\pi R/v$ and $\delta(t)$ is the impulse function.

By expressing (1.1) as a Fourier series, we can write

$$\lambda(t) = \frac{e}{vT_0} \sum_{n=-\infty}^{\infty} \exp(jn\omega_0 t) = \frac{e}{2\pi R} \sum_{n=-\infty}^{\infty} \cos(n\omega_0 t). \quad (1.2)$$

The frequency spectrum is obtained by the Fourier transform :

$$\Lambda(\omega) = \frac{e\omega_0}{2\pi v} \sum_{n=-\infty}^{\infty} \delta(\omega - n\omega_0).$$

The line at $n=0$ is the DC component of the signal, the remaining lines are successive orbital harmonics spaced by ω_0 . Since $\cos(-n\omega_0 t) = \cos(n\omega_0 t)$, the negative frequency lines are indistinguishable from those at corresponding positive frequency; the combined amplitude is thus twice the DC component.

If the velocity is close to that of light, as it is the case for relativistic particles, the electric and magnetic field accompanying the particle are confined in a thin pancake perpendicular to the direction of motion, with angular extent $1/\gamma$, where γ is the ratio of particle energy to the rest energy, resembling the TEM field distribution in a coaxial line.

A longitudinal pick-up couples to the particle fields, delivering a signal proportional to the linear charge density, whose harmonic content copies that of (1.2) (except that there is no induced DC signal) at least up to frequencies of the order $\approx \gamma c/b$, with b the effective radius of the beam pipe and c the speed of light, after which, due to the opening angle of the fields, cut-off occurs.

1.1.2 Transverse

A suitable configuration of pick-up's forms a beam position monitor (BPM), used to measure the horizontal or vertical transverse displacement from the design orbit. We use z to indicate the generic transverse position. A BPM is usually sensitive also to the current intensity so that the measured quantity is actually proportional to the *linear dipole density* d , defined as the product of the linear charge density λ times the position z .

$$d = \lambda \cdot z .$$

Let's write the position z as the superposition of two terms

$$z(t) = z_0 + \hat{z} \cos(\omega_\beta t) , \quad (1.3)$$

where z_0 is a stable offset due, for example, to a closed orbit distortion or to a BPM misalignment, or both, and the second term is the oscillatory one, due to the betatron oscillation, with $\omega_\beta = Q\omega_0$ the betatron angular frequency and Q the betatron tune.

The resulting linear dipole density is then obtained by multiplying (1.2) by (1.3)

$$d = z_0 \frac{e}{2\pi R} \sum_{n=-\infty}^{\infty} \cos(n\omega_0 t) + \hat{z} \frac{e}{2\pi R} \sum_{n=-\infty}^{\infty} \cos(n\omega_0 t) \cos(\omega_\beta t) . \quad (1.4)$$

The first term in (1.4) gives terms similar to (1.2) in the frequency content, but weighted by the closed orbit. The second term has a different signature and contains information on the betatron motion. If this latter is of interest, the closed orbit term is rejected by electronic means, or by centering the beam or even by centering the BPM itself [4, 5].

By considering only the second term in (1.4), the linear dipole density is written as

$$d = \hat{z} \frac{e}{2\pi R} \sum_{n=-\infty}^{\infty} \cos[(n + Q)\omega_0 t] , \quad (1.5)$$

showing the appearance of a whole set of side-bands beside the harmonics of the revolution frequency, produced by the non-linear operation of sampling the betatron motion at finite intervals of time.

It is interesting to express (1.5) in terms of positive frequencies only, as seen with a conventional spectrum analyzer (remember that frequency differ from angular frequency by the numerical factor 2π). To this purpose we first write $Q = M + q$, with M the integer part and q the fractional part of Q , and obtain

$$d = \hat{z} \frac{e}{2\pi R} \left\{ \cos(q\omega_0 t) + \sum_{n'=1}^{\infty} \cos[(n' \pm q)\omega_0 t] \right\}, \quad (1.6)$$

where the new index $n' = n + M$ has been introduced.

The components of the spectrum (1.6) with $+q$ are called *fast waves*. Those with $-q$ are called *slow waves*. If the value of q is less than $1/2$ ("above the integer") the fast waves stand at the high-frequency sides of the revolution harmonics and the slow waves at the low-frequency sides; when q is greater than $1/2$ ("below the integer") the opposite relationship holds.

Examining (1.6), we see that a whole set of ghost frequencies or *aliases* at distance $\pm q\omega_0$ from the revolution harmonics, plus a low-frequency line near DC (base-band) at $q\omega_0$ appear in the BPM spectrum. Therefore the measurement of the betatron spectrum with a spectrum analyzer (actually by any instrument, as long as we use a single BPM) only determines the fractional part q of the tune; the information about the integer part of the tune is lost.

This ambiguity is a consequence of under-sampling the betatron oscillation, so that we are not able to reconstruct the original signal from the information contained in the sampled data. Indeed, Shannon's sampling theorem [6] states that one can reconstruct exactly a sampled wave-form provided that the sampling frequency is at least twice higher than the highest frequency content in the original wave-form. In our case sampling occurs at the revolution frequency and the frequency of the betatron oscillation is Q times larger than the sampling frequency.

It is worth pointing out that if we replace the BPM by a device which kicks the beam transversally at each passage, any frequency appearing in the observed betatron spectrum can be resonantly excited.

1.1.3 Longitudinal Spectra with Synchrotron Satellites

In the presence of the longitudinal focusing produced by an RF accelerating field, a particle beam is bunched and the single particle undergoes synchrotron oscillations of the instantaneous energy.

The angular frequency of revolution is affected according to

$$\frac{d\omega}{\omega_0} = - \eta \frac{dp}{p_0}, \quad (1.7)$$

where $d\omega$ is the frequency variation, dp is the instantaneous momentum deviation with

respect to the nominal value p_0 and η is defined by

$$\eta = \left(\frac{1}{\gamma_t^2} - \frac{1}{\gamma^2} \right), \quad (1.8)$$

with γ_t the transition energy at which the increase of velocity corresponding to a momentum increase is compensated by the increase of orbit length, thus leaving the revolution time unaltered. The term $(1/\gamma)^2$ is called the *momentum compaction factor* α_c . At ultra-relativistic energies the second term in (1.8) becomes negligible and (1.7) is written

$$\frac{d\omega}{\omega_0} \approx - \alpha_c \frac{dp}{p_0}.$$

The time between successive passages measured at the monitor is

$$T_0 + \tau = T_0 \left[1 + \frac{\tau_s}{T_0} \cos(\Omega_s t + \psi) \right], \quad (1.9)$$

where Ω_s is the angular frequency of the synchrotron oscillation, ψ is a phase constant, τ_s is the amplitude of time-modulation and

$$\left(\frac{\Delta\tau}{T_0} \right) = - \left(\frac{d\omega}{\omega_0} \right) \approx \frac{d\tau}{dt} \quad (1.10)$$

In this case the linear charge density is

$$\lambda(t) = \frac{e}{v} \sum_{k=-\infty}^{\infty} \delta(t - kT_0 - \tau).$$

Using

$$\exp [jx \cos(y)] = \sum_{m=-\infty}^{\infty} (j)^m J_m(x) \exp(jmy)$$

and (1.2), we can express the linear charge density as a Fourier series

$$\lambda(t) = \frac{e}{2\pi R} \sum_{n,m=-\infty}^{\infty} (-j)^m J_m(n\omega_0\tau_s) \exp j [(n\omega_0 + m\Omega_s)t + m\psi]. \quad (1.11)$$

Each original line in the spectrum (1.2) has now degenerated into an infinite set of satellites right and left at $\pm\Omega_s, \pm 2\Omega_s, \dots, \pm m\Omega_s$ with the amplitudes modulated by the Bessel functions of the first kind of order m, J_m .

The argument $n\omega_0\tau_s$ corresponds to the phase-modulation index used in telecommunications. Although there is a nominally infinite number of side-bands, only a finite number are of appreciable amplitude: namely the higher order coefficients $J_m(n\omega_0\tau_s)$ fall-off very rapidly beyond $m \sim n\omega_0\tau_s$ (see Fig. 1).

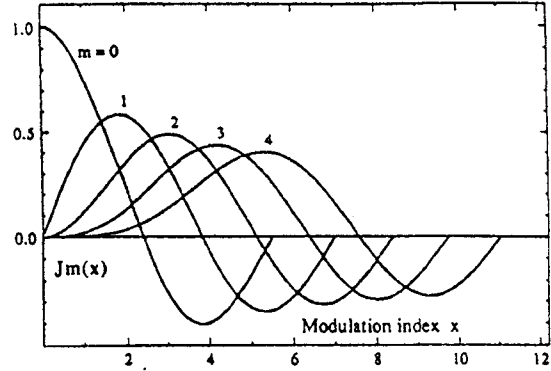


FIG. 1 - Qualitative sketch of the behavior of the Bessel function $J_m(x)$.

1.1.4 Transverse Spectra with Synchrotron Satellites

If we now go back to the betatron motion, we must also take into account the modulation of the betatron tune due to the energy modulation. In fact, the machine lattice focuses differently particles with energy deviating from the nominal value. The chromaticity of a machine is defined as the relative change in tune of a particle with relative momentum deviation dp

$$\xi = \text{chromaticity} = \frac{dQ}{dp} \cdot \frac{p_0}{Q_0}, \quad (1.12)$$

where Q_0 is the tune value pertaining to the nominal energy.

According to the above definition, the rate of change of the betatron phase μ_β in the presence of energy oscillations is then, to first order,

$$\dot{\mu}_\beta = \omega_\beta = \omega_0 Q_0 \left(1 + \frac{d\omega}{\omega_0} + \frac{dQ}{Q_0} \right) = \omega_0 Q_0 \left[1 - \frac{\tau}{T_0} \left(1 - \frac{\xi}{\eta} \right) \right] \quad (1.13)$$

and, taking into account the time dependence (1.9) of the time of passage and its rate of change (1.10), the betatron phase is

$$\mu_\beta(t) = \omega_0 Q_0 t + (\omega_\xi - \omega_0 Q_0) \tau_s \cos(\Omega_s t + \psi), \quad (1.14)$$

where the chromatic frequency $\omega_\xi = (\xi Q_0 / \eta) \omega_0$ has been introduced.

The expression of the linear dipole density d is now written, taking into account (1.11) and (1.14), as

$$d(t) = \frac{e \hat{z}}{2\pi R} \sum_{n,m=-\infty}^{\infty} (-j)^m J_m \left\{ \left[(n+Q)\omega_0 - \omega_\xi \right] \tau_s \right\} \exp[j(\omega_{nm} t + m\psi)], \quad (1.15)$$

with the *mode frequency* $\omega_{nm} = (n+Q)\omega_0 + m\Omega_s$.

Here we have again infinite synchrotron satellites around the betatron lines, but, due to the tune modulation (1.13), the amplitude envelope function is shifted by the chromatic frequency w_x . Thus, examining with a spectrum analyzer (positive frequencies only) the slow and fast waves straddling a harmonic of the revolution frequency, the mode amplitudes above and below may be quite different due to the different argument of the modulating Bessel function. Namely, across the high and low frequency sides of the n -th revolution harmonic the satellites amplitude is modulated by:

$$\begin{aligned} \text{Fast waves} &\rightarrow \left| J_m \left\{ \left[(n+q)\omega_0 - \omega_\xi \right] \tau_s \right\} \right| \\ \text{Slow waves} &\rightarrow \left| J_m \left\{ \left[(n-q)\omega_0 + \omega_\xi \right] \tau_s \right\} \right|. \end{aligned}$$

1.2 Many Particles

1.2.1 Schottky Noise

So far we have considered the somewhat idealized case of a single particle. If we turn to the realistic situation, many particles should be considered.

In a coasting beam the particles are randomly distributed around the machine and the time average of spectra (1.2) over all the particles is null, except for the DC component, i.e. the average current. On the other hand, if we take the RMS average of the spectrum over a finite bandwidth in frequency domain around a revolution harmonic, a signal of finite power results from the statistical fluctuations of the large, though finite, number of particles [3, 7, 8]. This is called the *Schottky noise signal* and its average power per observation bandwidth is proportional to the number of particles N . Figure 2 shows an example of Schottky spectrum measured at Cern-ISR [7].

The power density of a Schottky band is inversely proportional to the spread in the revolution frequencies; if η is known, momentum spread can be inferred from frequency spread.

The frequency spread in the transverse Schottky signal contains contributions from both the spread of revolution frequencies and from the tune spread due to the chromaticity, which can then be evaluated. The signal level of the transverse Schottky bands is however much lower than in the longitudinal case, requiring tuned detectors and the use of very low-noise electronics.

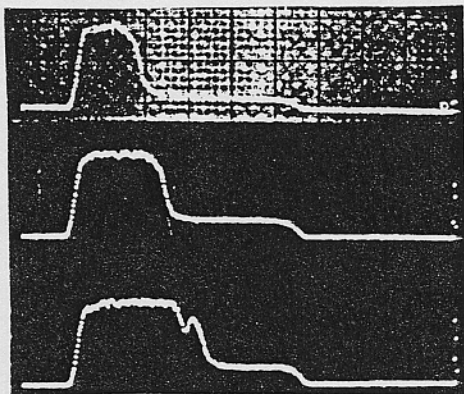


FIG. 2 - Longitudinal Schottky scan [7].

In the case of bunched beams, the transverse Schottky signal is also present, but the so called *common-mode* (first term in eq. 1.4) signal power, proportional to N^2 , tends to obscure it and makes the observation troublesome. Then, very selective filtering and careful mechanical centering of the BPM around the beam is required. A transverse detector for bunched proton beams, implemented at Cern-SPS, has been described in Ref. [4]. In a transverse Schottky noise detector used for stochastic cooling at Fermilab-Tevatron [5], optical correlator filters with deep periodic notches at the revolution harmonics are used to reject the strong common mode signals.

In the same way as there are synchrotron satellites in the single particle spectra (1.11, 1.15), in the Schottky spectra of a bunched beam each revolution line in the longitudinal signal and each betatron line in the transverse splits into an infinite number of synchrotron satellites (see Fig. 3). Thus, any incoherent frequency shift or spread of the synchrotron frequency can be measured.

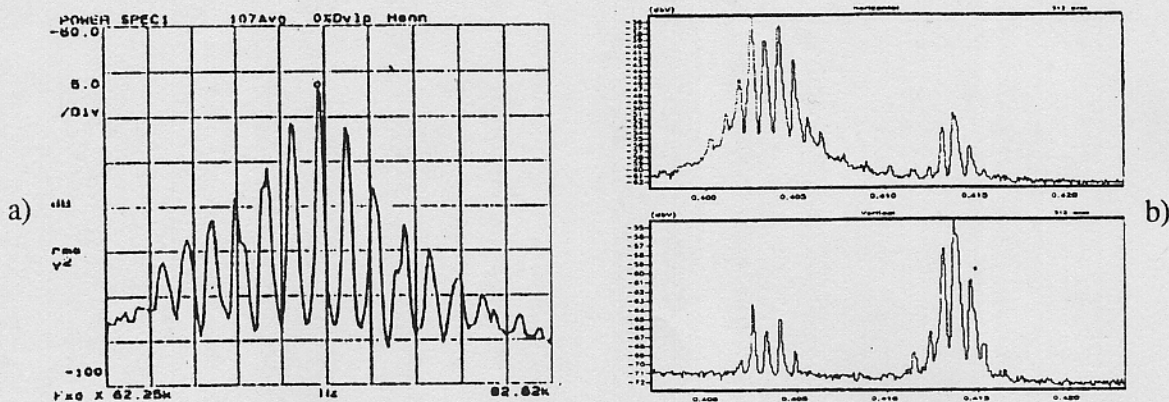


FIG. 3 - Schottky spectra exhibiting synchrotron satellites. a) Longitudinal [10] - b) Transverse [11].

1.2.2 Single Bunch

A great deal of information about the accelerator environment can be obtained through the study of the spectrum of coherent modes of a bunch of particles. A rigorous analysis of the modes and coherent patterns in the phase space can be found in [2]. Here we limit ourselves to qualitative considerations concerning the mode spectra.

Let us start with longitudinal coherent modes. The actual beam can be considered as a beam with a stationary distribution $g_0(\tau_s)$ in the longitudinal phase-space, plus some small density modulation Σg_m , which always exists due, for example, to previous beam manipulations such as injection and bunching for protons, and in general, to the interaction with the machine impedances:

$$g_m(\tau_s, \phi) = R_m(\tau_s) e^{jm\phi} \quad (1.16)$$

Here we consider the longitudinal phase-space of phase and amplitude coordinates ϕ - τ_s , in which the trajectory associated with the unperturbed motion is a circle. Each pattern g_m rotates in the longitudinal phase space at a frequency $m\Omega_s + \Delta\omega_{lm}$, where $m=1$ for dipole modes, $m=2$ for quadrupole modes, $m=3$ for sextupole modes, etc. $\Delta\omega_{lm}$ is a coherent frequency shift, depending, for example, on bunch current, machine impedance, feedback system and bunch length.

The resulting signal is the sum of the stationary distribution and of the perturbations g_m . The frequency spectrum of the stationary distribution is a line spectrum at harmonics of the revolution frequency, peaked at zero frequency and extending over $\sim \pm 2\pi/\Delta\tau$ rad/sec, where $\Delta\tau$ is the full bunch length. For example, in the case of a gaussian distribution with standard deviation σ , the full length is taken as 4σ . Power spectra envelopes corresponding to various linear charge densities within a bunch are shown in Fig. 4.

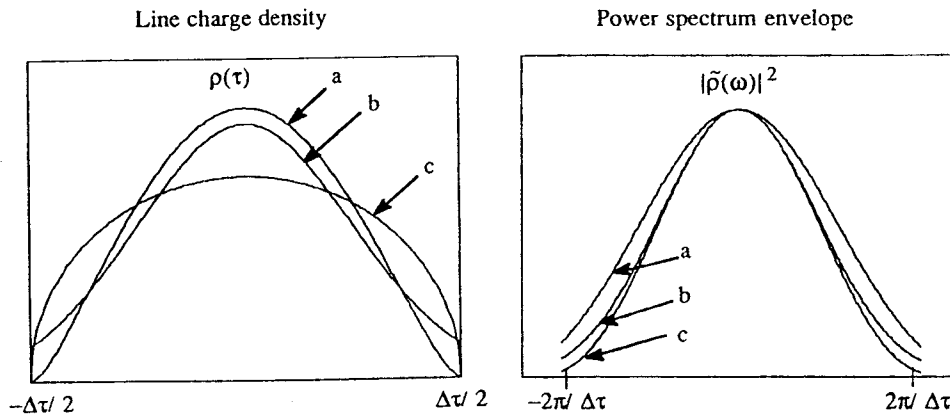


FIG. 4 - Line densities and corresponding power spectra for various stationary distributions: a) Parabolic amplitude density - b) Gaussian amplitude density - c) "Water-bag" bunch.

The coherent modes show a line spectrum at frequencies

$$\omega = n\omega_0 + m\Omega_s + \Delta\omega_{lm} \quad [- \infty \leq n, m \leq \infty] .$$

The m -th mode corresponds to $m+1$ half wavelength of a line density modulation along the bunch.

The spectrum of such a perturbation has a broad maximum at $\omega_m \sim (m+1)\pi/\Delta\tau$ (see Fig. 5) and extends over a frequency range of $\Delta\omega \sim \pm 2\pi/\Delta\tau$.

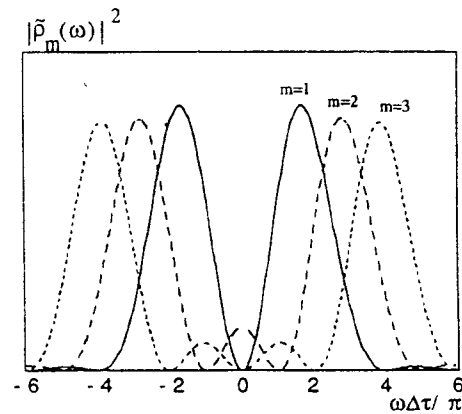


FIG. 5 - Envelopes of the frequency spectra of modes $m=1,2,3$.

For the transverse case we have a line spectrum at angular frequencies:

$$\omega = (n + q)\omega_0 + m\Omega_s + \Delta\omega_{lm} \quad [- \infty \leq n, m \leq \infty] ,$$

where $\Delta\omega_{lm}$ is a coherent frequency shift. Some differences in the spectrum of the transverse signal should be mentioned with respect to the longitudinal one:

- the transverse signal induced by a stationary distribution is null;
- a coherent transverse mode $m=0$ exists, corresponding to a dipolar transverse oscillation of the center of mass of a bunch with a stationary distribution in the longitudinal phase space; on the other hand, there are not longitudinal coherent modes at $m=0$;
- the spectrum amplitude is peaked at ω_ξ for mode $m=0$ and $\omega_\xi \pm (m+1)\pi/\Delta\tau$ for other modes.

1.2.3 Many Bunches

A beam, consisting of M similar and equally-spaced bunches can oscillate coherently in M different modes, depending on the phase relationship between the individual oscillations. In order to look for suitable phase shifts between the density perturbations of adjacent bunches we consider the over-simplified situation of M equal bunches consisting of one particle on the same phase-space orbit of radius τ_s . Then the linear charge density is

a sum of M contributions :

$$\lambda(t) = \frac{e}{v} \sum_{b=1}^M \sum_{k=-\infty}^{\infty} \delta \left[t - \left(\frac{b}{M} + k \right) T_0 - \tau_b \right], \quad (1.17)$$

where

$$\tau_b = \tau_s \cos \left(\Omega_s t + \psi_b \right).$$

Proceeding in the same way as in (1.2) and (1.11), we get the result (1.18) below :

$$\lambda(t) = \frac{e}{2\pi R} \sum_{n,m=-\infty}^{\infty} (-j)^m J_m(n\omega_0 \tau_s) \exp \left[j(n\omega_0 + m\Omega_s) t \right] \sum_{b=1}^M \exp \left[j \left(m\psi_b - \frac{2bn\pi}{M} \right) \right].$$

The last Σ is equal to M provided that the phase shifts between the perturbations of two adjacent bunches satisfy

$$m(\psi_{b+1} - \psi_b) = \frac{2p\pi}{M}, \text{ modulo } 2\pi, \quad (1.19)$$

where p can be 0, 1, 2, ..., $M-1$, defining the p -th mode of coherent coupled bunch motion.

When (1.19) is not fulfilled the last Σ in (1.18) is equal to zero. So, for M similar bunches, M distinct *longitudinal* coherent coupled bunch modes can be excited. The spectrum of the p -th mode is at frequencies:

$$\omega_k = (kM + p)\omega_0 + m\Omega_s,$$

with k running from $-\infty$ to $+\infty$. The amplitude of the spectrum lines is M times larger than in (1.11), but M times more spaced in frequency.

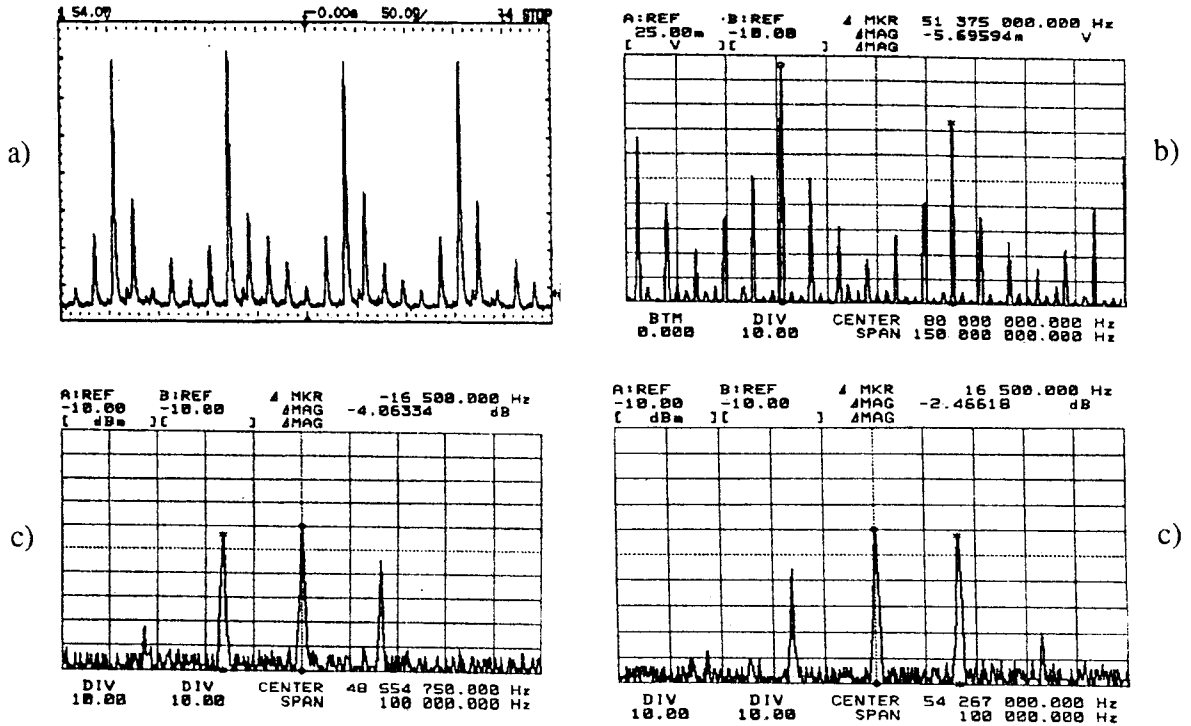
It can be shown also for the *transverse* motion that for M equally spaced bunches, only every M -th line occurs for every p -th coupled mode:

$$\omega_k = (kM + p + Q)\omega_0 + m\Omega_s,$$

where, again, $p = 0, 1, \dots, M-1$ and $-\infty \leq k \leq +\infty$.

If the bunches carry unequal charges or they are not equally spaced we see a more complicated line pattern (see Fig 6).

ADONE : Revolution Time $T_0 = 350$ ns ; minimum bunch spacing = $T_0/18$



SPEAR : Revolution Time $T_0 = 781$ ns ; minimum bunch spacing = $T_0/140$

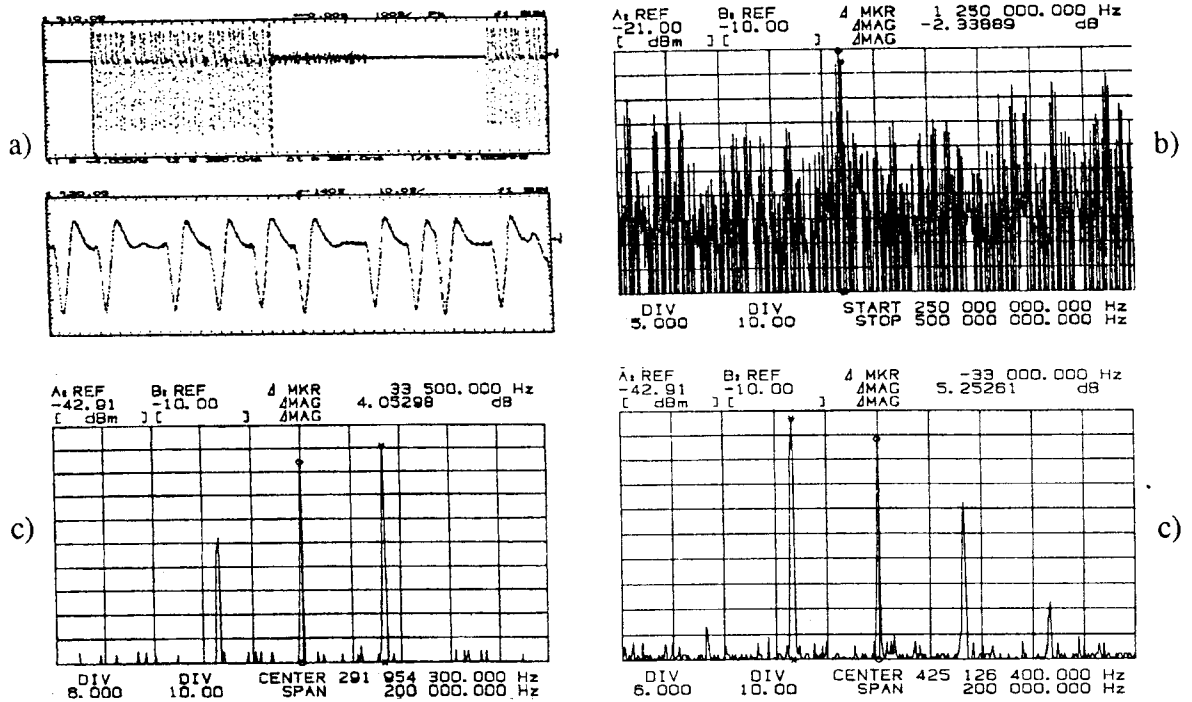


FIG. 6 - Unequally populated bunches at ADONE (upper half) and SPEAR (lower half). a) Time structure; b) Broad-band spectrum; c) Sideband spectra of longitudinal coherent coupled bunch modes $p=1$ and 17 for ADONE and $p=52$ and 88 for SPEAR.

2. BEAM PICK-UP'S AND KICKERS

In the following sections we briefly review various types of beam pick-up's and kickers and remark some peculiarities. The literature about beam instrumentation is abundant: we cite as general reference the excellent reviews by Littauer [1], Borer-Jung [12] Pellegrin [13] and the essay by Lambertson-Goldberg [14].

2.1 Beam Pick-up's

In its simplest conception, a non-intercepting beam pick-up can be thought of as a discontinuity in the vacuum chamber of an accelerator, which interrupts and diverts into a measuring device a portion of the wall image-current associated to the beam.

The frequency response of such a simplified monitor in principle can extend to a very high frequency. The pick-up transfer characteristics include the effects of the beam distance from it. Hence, by a suitable combination of pick-up's signals, it is possible to extract information about the longitudinal beam profile or its transverse position.

For example, by adding the signals from diametrical pickup's, one can remove the dependence on the transverse position and retain the intensity information. On the other hand, one can measure the linear dipole density (Beam Position Monitor), by subtracting the signals from two opposing pick-up's (see Fig. 7). The difference signal can be normalized to the sum signal, to remove the dependence on current intensity. The difference can be made directly at the BPM, e.g.: by means of wide-band hybrid junctions, or by digitizing the single p.u. signals and computing later the beam position by extrapolation from a calibration table.

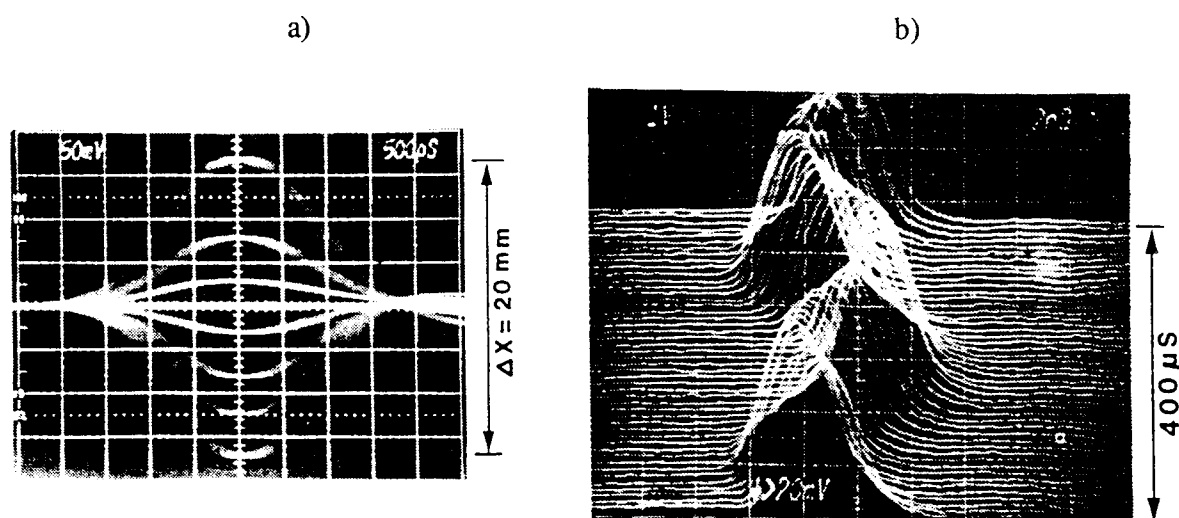


FIG. 7 - a) Superposition of signals for various horizontal positions by the difference connection of two ports of a wall-current monitor - b) "waterfall" display of longitudinal coupled bunch oscillations by the sum connection of four ports of the same monitor (from ref. [15]).

There is a virtually unlimited variety of beam monitors around the accelerators and we are not going to make a description nor a classification. However, it is interesting to discuss with some detail the *strip-line* monitor [1, 3, 12-14, 16].

The strip-line is an electrode, usually longer than the characteristic bunch length, which forms with the vacuum pipe a transmission line of characteristic impedance Z_0 . By a suitable choice of the ratio between the strip width and distance from the pipe, the characteristic impedance is made 50Ω . The electrode is terminated at both ends via coaxial vacuum feed-through's into termination loads matched to Z_0 (see Fig. 8).

In the strip-line monitor both the electric and the magnetic field contribute to the output signal but the beam electromagnetic field and the wave field in the transmission line interfere constructively at one port and destructively at the other yielding directional properties.

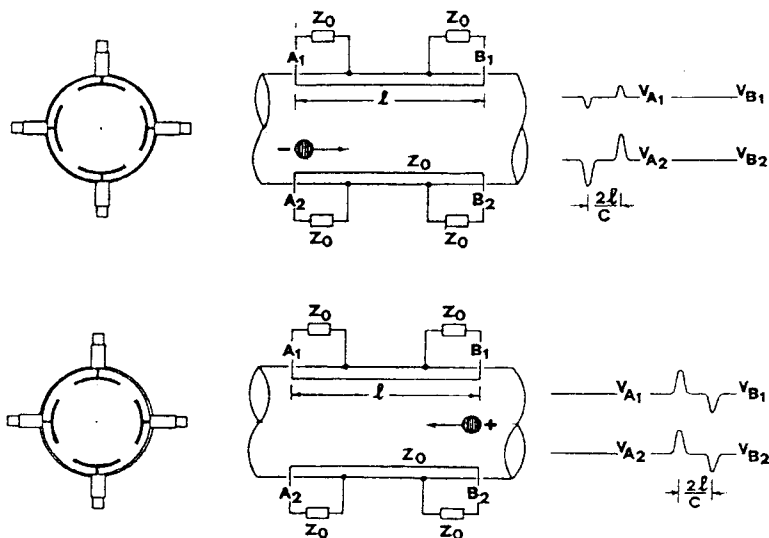


FIG. 8 - Schematic representation of a directional strip-line monitor with beams of opposite velocity and charge. Qualitative sketch of the voltages at the output ports.

In principle we get an useful signal only at the up-stream port of the monitor. The voltage at the up-stream load resistor is a doublet of pulses of opposing polarity reproducing the longitudinal time distribution of the beam current and separated in time by an interval $\Delta t = 2l/c$, where l is the strip length. No signal appears at the down-stream port as long as the beam velocity and the propagation velocity in the strip are equal (this means ultra-relativistic beam and a minimum or null amount of dielectric in the vicinity of the strip) and the load resistor is exactly matched to the line impedance. In practice any impedance mismatch introduced, for example, by the vacuum feed-through's or by mechanical imperfections, tends to spoil the directional properties of the monitor.

The directionality of the strip-line monitor is particularly useful with colliding beams, if one wants to measure only one beam position in presence of the other beam.

The time-domain voltage response of the matched strip-line is, at the up-stream port and for a centered beam

$$v(t) \approx \frac{Z_0}{2} \left(\frac{\alpha}{2\pi} \right) \left[i_b(t) - i_b\left(t - \frac{2l}{c}\right) \right] ,$$

with α the opening angle of the strip, $(\alpha/2\pi)$ the factor of coverage and $i_b(t)$ the instantaneous beam current. The strip-line coupling impedance in the frequency domain is

$$Z_c(j\omega) \equiv \frac{V(j\omega)}{I_b(j\omega)} \approx Z_0 \left(\frac{\alpha}{2\pi} \right) \sin\left(\frac{\omega l}{c}\right) e^{j\left(\frac{\pi}{2} - \frac{\omega l}{c}\right)} ,$$

where $V(j\omega)$ and $I_b(j\omega)$ are the spectral densities of the output voltage and of the beam current. The response is maximum at frequency $f = c/4l$, or odd multiples, and zero at $f = c/2l$, or multiples.

The position sensitivity of a pair of difference-connected strip-lines to a small beam displacement Δz from the center line is

$$\frac{b}{2} \frac{\Delta V}{\Sigma V} \approx \Delta z ,$$

where ΔV is the difference voltage of two opposing strips, ΣV is the sum voltage and b is the vacuum chamber radius.

Starting from the strip-line we can think of some variations:

- Electrostatic monitor. A short, unterminated strip, in the form of a plate, with an outside connection in the middle (think, for example, of a button monitor) is no longer a directional device and is mainly sensitive to the beam electric field. The usual equivalent circuit representation of an electrostatic monitor is a current generator of the same value of the portion of the image current intercepted, shunted by the electrode capacitance to ground.
- Magnetic monitor. A strip, shorted to the vacuum chamber at the other side of the output port, forms a loop and is mainly sensitive to the beam magnetic field [17]. The equivalent circuit of a magnetic loop is a voltage generator with a series inductor. The voltage is proportional to rate of variation of magnetic flux associated with the beam current and linked to the loop, the series inductance is the loop self-inductance.

It is then possible to obtain a tuned (narrow-band) monitor by making the plate or loop part of an L-C resonant circuit. The sensitivity can be very high, at the expenses of a bandwidth reduction.

We mention beam size monitors here because they can give useful information about the coherent and incoherent increase of transverse dimensions. The favourite beam dimension monitor, at least at electron facilities, is the *synchrotron radiation monitor*. Due to the high directionality of the synchrotron radiation, the spatial distribution of the emitted light reproduces fairly well the transverse distribution of charge density in the beam. By projecting the light onto some slit [18] or pinhole, followed by a photodetector, or onto a linear array of photodiodes, an accurate measurement of the charge density can be obtained.

2.2 Kickers

Longitudinal or transverse kickers are used to excite coherent oscillation modes by the application of a rapidly varying external field.

By phase-modulating the voltage in an RF cavity it is possible to drive longitudinal dipole oscillations of a bunch. By amplitude-modulation of the RF voltage, longitudinal quadrupole oscillations can be excited, provided that the cavity bandwidth extends over the mode frequency.

We can turn a matched strip-line into a longitudinal kicker by applying in-phase deflecting voltages at the down-stream ports. By entering the strip-line region, the beam will receive a longitudinal kick because the strips are at non-zero potential. If the driving frequency is $c/4l$, by the time the beam traverses the strips, the voltage at the down-stream port will have reversed, causing another longitudinal kick in the same direction. The frequency response of a strip-line longitudinal kicker is the same as for the stripline monitor, i.e. : broadly resonating at frequencies $c/4l$, or odd multiples.

Strip-lines can also be used as transverse kickers, maintaining the directional properties described in section 2-1. Two voltages of opposing polarity are applied down-stream the beam direction at facing ports. The combined magnetic field, due to the current flow along the strip, and electric field, due to the strip potential, give a net deflecting Lorentz force in the transverse plane identified by the strips, all along their length (see Fig. 9). The electric and magnetic forces cancel if the power flow is in the same direction as the beam velocity. Then, in the case of colliding beams, it is possible to excite selectively one beam without effect on the other.

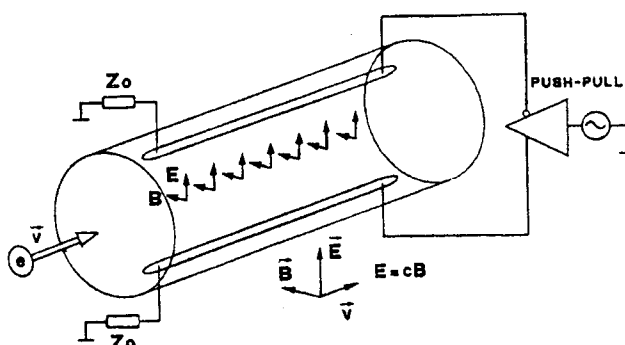


FIG. 9 - Strip line transverse kicker.

The useful bandwidth is relatively large: in fact the efficiency as a function of frequency is proportional to $\propto \frac{\sin(\omega l / c)}{(\omega l / c)}$ and retains the directional properties down to

frequencies where the skin depth becomes larger than the thickness of the vacuum chamber wall and the magnetic field starts leaking out of the pipe. The kicker efficiency is zero at frequencies $f = c/2l$ or multiples, because the deflecting force encountered in the strip-line region is in one direction for half a transit time and in the opposite direction for the other half.

In the same way as BPM's are sensitive to electric or magnetic field, we can deflect a beam electrically by open plates driven by a voltage generator, or magnetically, by coils driven by a current generator.

The capacitor formed by the plates and the inductor formed by the coils can be part of an L-C resonant circuit to reduce the power requirement of the driving amplifier.

We remark that, by combining several strip-lines in series with $\lambda/2$ delay lines [14], it is possible to increase the sensitivity/strength at the peak frequency at the expense of a reduction of the bandwidth, but leaving the source/load impedance constant.

3. BEAM RESPONSE MEASUREMENTS

In this section we describe measurements of the beam response correlated with external excitation and their various uses.

We have seen that, thanks to the Schottky noise, it is possible to detect small incoherent oscillations within a beam of particles; if a beam is executing coherent oscillations of some kind, passive observation of the modes is generally possible but sometimes these oscillations have a transient behaviour, and are difficult to catch.

For the systematic study of the longitudinal and transverse spectra, it is often useful to excite some oscillation mode of the beam in a steady way or with a shock excitation (all modes simultaneously) by means of a longitudinal or transverse kicker, and observe the beam response by means of some pickup. We call this class of measurements *stimulus-response*.

As in linear circuit theory, the beam response may be analyzed either in the time domain or in the frequency domain. The two methods are mathematically equivalent: the pulse and frequency response being related to each other by a Fourier transform pair.

3.1 Shock Excitation

Measuring the beam response to a shock excitation corresponds to studying the transient response of a circuit to a delta pulse. This method is often used to observe the evolution of transverse modes. The stimulus is provided by a fast transverse force produced by a kicker magnet and lasting for a time less than a revolution period, which excites coherent transverse oscillations. An injection kicker is sometimes used for this purpose. The response is the beam transverse position detected by a beam position monitor.

If there is provision for single-turn beam position measurement, it is possible to sample and digitize with a fast ADC the beam position at one or several monitors, and perform a numerical Fourier analysis on the sampled data to obtain, for example, the fractional tune value and its distribution [19], or the betatron phase advance between two azimuthal positions [20].

A shock excitation drives at the same time all coherent modes of oscillations. A conventional spectrum analyzer operating in the zero-span mode can be used as a tuned detector at a fixed frequency to selectively measure the damping or growth rate of individual head-tail modes as a function, for example, of the chromaticity or of the current intensity [1].

It is noteworthy that, when measuring with the kick method, the observation time and, therefore, the ultimate accuracy of the measurement are limited by the damping.

3.2 Continuous Excitation

In frequency-domain measurements, the stimulus to the beam is a CW longitudinal or transverse force provided by a kicker driven by a swept or fixed frequency sinusoidal generator and the response is the amplitude of the resulting oscillation.

By exciting transversely a beam with a frequency close to a betatron side-band and measuring turn by turn the beam position at several monitors over many successive passages, it is possible to de-embed from the relative phases and amplitudes the betatron phase advance and the local values of the beta-functions. This method has been recently used at LEP [21]. By exciting a steady synchrotron oscillation and applying the same analysis, the local values of the dispersion function could be measured.

A basic tune measurement system can be made with a swept spectrum analyzer and a tracking generator or with a network analyzer. The tracking generator is a sinusoidal RF source whose output frequency exactly follows that instantaneously displayed at the spectrum analyzer. A network analyzer provides itself an RF output and measures the gain ratio and the relative phase between excitation and response altogether. The RF output is used to drive a kicker and the signal from a beam monitor is fed to the instrument to measure the beam response (complex, with the network analyzer). The kicker and the detector can be part of a feedback system, where available. In some measurements the response of the transverse beam density is measured with a beam size monitor (see Fig. 10) [18].

Due to the longer observation time allowed, the frequency resolution is finer than with the kick method, on the other hand the direct perception of damping is lost. The tradeoff between the frequency accuracy Δf and the observation time Δt is imposed by the indetermination relation $\Delta f \geq 1 / \Delta t$ [6].

In colliding beam machines two normal modes of oscillations exist. The mode with the two beams oscillating in-phase is called the sum, zero, or σ -mode, the other, with out-of-phase oscillations, is called the difference or π -mode. The frequency of the σ -mode is equal to that of the single beam, because there is not relative motion, while the frequency of the π -mode is shifted because of the additional focusing by the beam-beam force and spread because of the non-linearity of such forces. This effect is related to the incoherent beam-beam tune-shift and is used to characterize the beam-beam interaction.

```
DATA 28/05 ORE 18.11
FASCIO DI ELETTRONI (3 BUNCHES): Ibeam=25 mA
ENERGIA = 1400 MeV ; tau damping = 14 msec
CORRENTE NEI Q-POLI "F" ; 352 Amp.
CORRENTE NEI Q-POLI "D" ; 354 Amp.
TENSIONE DI RADIO-FREQUENZA ; 120 KV
AMPIEZZA TENSIONE DI ECCITAZIONE ; 3.1 Vpp      Twait = 41 msec
SWEEP UP
Qz = 3.1127
MASSIMO ALLARGAMENTO ; 34 %
SIDEBANDS DI SINCROTRONE ASSENTI
```

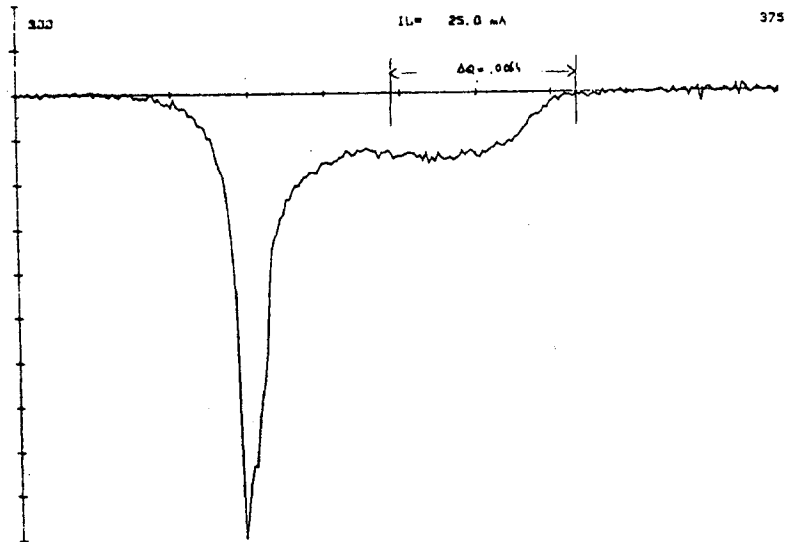


FIG. 10 - Vertical beam size response in the presence of trapped ions.

There is another effect, the *tune coupling* [22], which has been used very effectively to optimize the collision point of the HERA e-p collider with separate rings, and looks very attractive for the next generation high-luminosity factories. The basic idea is to make a cross measurement of one beam response when the other beam is excited. The beam response is at its maximum when the two beams overlap.

The *Beam Transfer Function* (BTF) can be measured with a network analyzer. Figure 11 shows a schematic layout of a transverse BTF measurement.

The response (amplitude and phase) of a coasting beam to an external longitudinal or transverse excitation has been used to extract information about the incoherent tune distribution, and about the forces generated by the beam interaction with the parasitic impedance of the machine and with feedback systems [1, 3, 8, 12, 23].

The same kind of measurement for bunched beams entails more subtleties. It has, however, been applied to examine the longitudinal quadrupole mode response of an electron beam [24, 25] and to test and characterize the effectiveness of an experimental longitudinal feedback system [26].

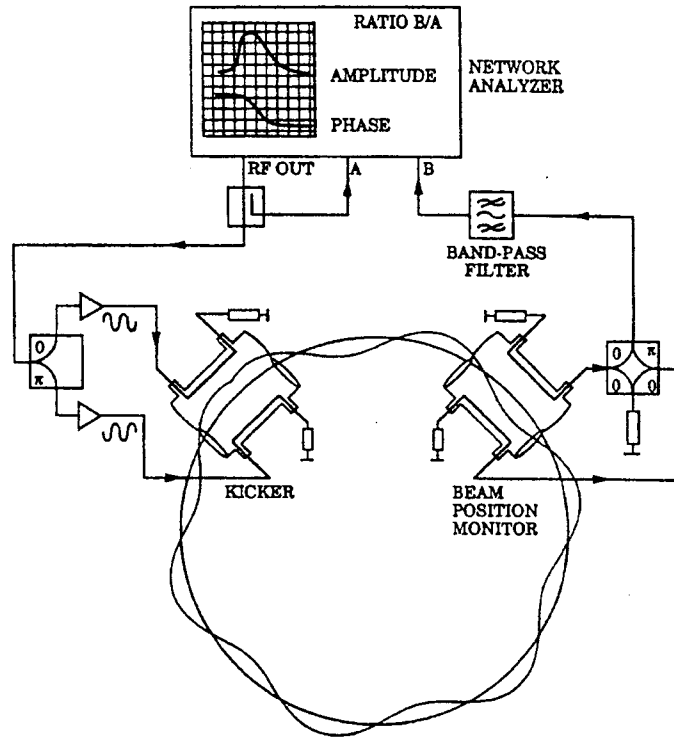


FIG. 11 - Schematic layout of a Beam Transfer Function measurement system.

3.3 Digital Analyzers

In the measurement with a conventional swept spectrum or network analyzer, due to the indetermination relation mentioned above and to the fact that a single frequency is analyzed at a time, a long observation time is involved. In addition to the intrinsic indetermination, every time we change the frequency we must allow the transient beam response to die-out and the steady-state response to be attained.

The problem can be overcome by the use of a *dynamic signal analyzer*, or *digital spectrum analyzer*, which is based on high-speed digital Fourier analysis (Fast Fourier Transform-FFT) executed by an embedded processor. N voltage samples over a period T are digitized and transformed into $N/2$ complex Fourier coefficients, spanning a frequency range from DC to $N/2T$, with a frequency resolution $\Delta f = 1/T$. The whole spectrum is available almost instantly, thus the total measurement time is reduced by a nominal factor $2/N$ with respect to a conventional swept analyzer with the same frequency resolution. The number of frequency points computed is typically ~ 200 to ~ 1000 with a real-time bandwidth (no dead-time or data loss between successive spectra computations) nowadays extending to ~ 100 KHz.

Such analyzers usually provide two independent channels for spectrum analysis, a pseudo-random noise generator and capability for complex transfer function calculations. In a BTF setup the noise output, applied to a kicker, excites all modes within the band at the same time. A modest power is enough to produce measurable oscillations without blowing-up the beam. The beam response is cross-correlated with the noise excitation and the complex beam transfer function is measured.

The relatively low operating frequency is no problem, as long as the band of interest is within the maximum frequency of the FFT analyzer. For example, the IF output of a conventional RF spectrum analyzer operating in the zero-span mode as a fixed frequency detector, can be mixed down to base-band and measured at narrow resolution bandwidth with the FFT analyzer.

In BTF measurements the noise output is up-converted to the frequency of the mode under study and the beam signal is down-converted to the operating frequency of the analyzer [8]. A schematic layout of a longitudinal BTF measurement system with a dynamic signal analyzer is shown in Fig. 12.

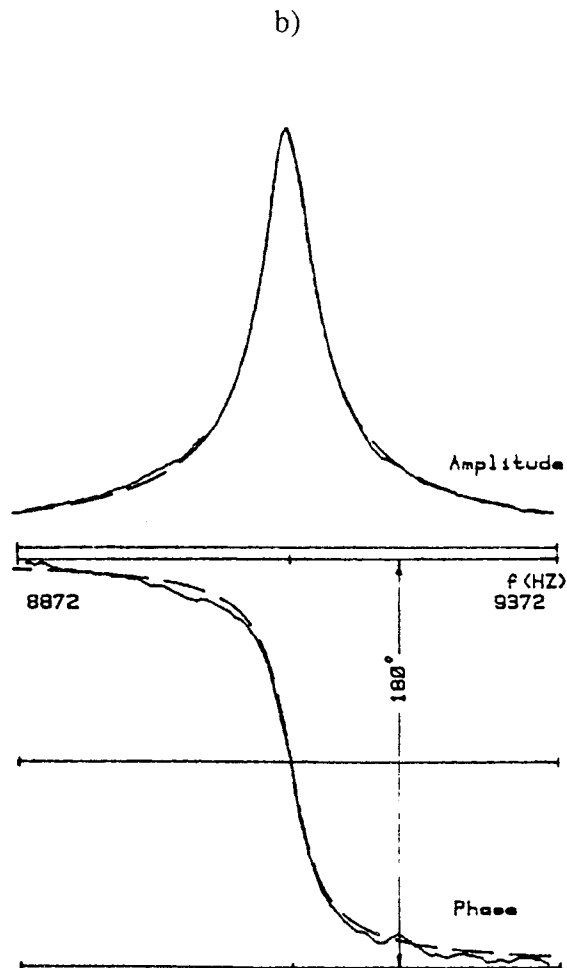
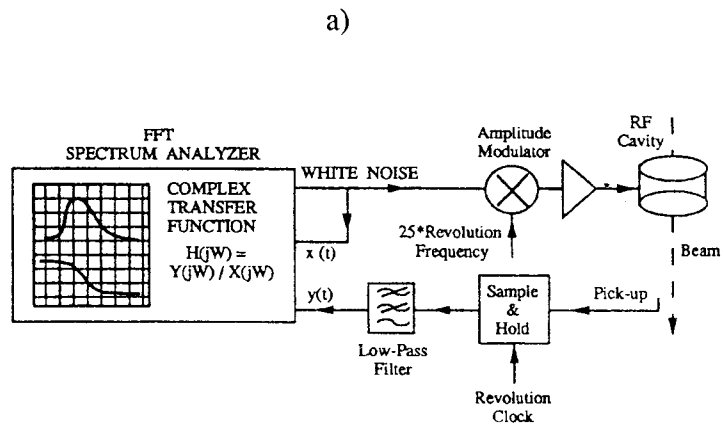


FIG. 12 - a) Schematic layout of a BTF measurement system with an FFT analyzer - b) Longitudinal BTF measurement (from ref. [25]).

REFERENCES

- [1] R. Littauer: "Beam Instrumentation", in "Physics of High Energy Particle Accelerators". Editor: M. Month - AIP Conference Proceedings No. 105, pp. 869-953 (1983).
- [2] J. L. Laclare: "Bunched Beam Coherent Instabilities", Cern Accelerator School - Advanced Accelerator Physics Course. Proceedings. Editor: S. Turner - CERN 87-03, p.264 (1987).
- [3] D. Boussard: "Schottky Noise and Beam Transfer Function Diagnostics", *ibid.*
- [4] T. Linnecar, W. Scandale: "A Transverse Schottky Noise Detector for Bunched Proton Beams", IEEE Trans. on Nuclear Science, Vol. NS-28, n.3, p. 2147 (1981).
- [5] G. Jackson et al. : "Bunched Beam Schottky Signal Measurements for the Tevatron Stochastic Cooling System", Proceedings of Advanced Beam Instrumentation Workshop, KEK-Proc. 91-2 (1991).
- [6] A. Papoulis: "The Fourier Integral and its Applications", Mc Graw-Hill Book Company, inc. (1962).
- [7] J. Borer et al. : "Non-destructive Diagnostics of Coasting Beams with Schottky Noise", Proceedings of the IX-th International Conference on High Energy Accelerators, Stanford, May 1974, p.53 (1974).
- [8] J. Borer et al. : "ISR Beam Monitoring System Using Schottky Noise and Beam Transfer Function", CERN-ISR-RF/80-30 (1980).
- [9] R. J. Pasquinelli et al. : "Optical Correlator Notch Filters for Fermilab Debuncher Betatron Stochastic cooling", Proceedings of the 1989 IEEE Particle Accelerator Conference, Chicago, March 1989, 89CH2669-0, p.694 (1989).
- [10] K. Beckert et al. : "The ESR Schottky-Diagnosis System", Proceedings of the 2-nd European Particle Accelerator Conference, Nice, June 1990, p.777 (1990).
- [11] D. Martin et al. : "A Schottky Receiver for Non-perturbative Tune Monitoring in the Tevatron", Proceedings of the 1989 IEEE Particle Accelerator Conference, Chicago, March 1989, 89CH2669-0, p.1483 (1989).
- [12] J. Borer, R. Jung: "Diagnostics", Cern Accelerator School - Antiprotons for Colliding Beam Facilities. Proceedings. Editors: P. Bryant, S. Newman - CERN 84-15, p.385 (1984).
- [13] J. L. Pellegrin: "Review of Accelerator Instrumentation", Proceedings of the XI-th International Conference on High Energy Accelerators, CERN, Geneva, July 1980, p.459 (1980), also Slac Note SLAC-PUB-2522 (1980).
- [14] D. A. Goldberg and G. R. Lambertson : "Dynamic Devices: A Primer on Pickups and Kickers", LBL-31664 (1991).
- [15] G. C. Schneider : "A 1.5 GHz Wide-Band Beam Position and Intensity Monitor for the Electron-Positron Accumulator (EPA)", Proceedings of the 1989 IEEE Particle Accelerator Conference, Chicago, March 1989, 89CH2669-0, p.664 (1989).
- [16] R. E. Shafer: "Characteristics of Directional Coupler Beam Position Monitors", IEEE Trans. on Nuclear Science, Vol. NS-32, n.5, p. 1933 (1985).
- [17] J. C. Denard et al. : "Parasitic Mode Losses versus Signal Sensitivity in Beam Position Monitors", Slac Note SLAC-PUB-3654 (1985).
- [18] M. E. Biagini et al. : "Observation of Ion Trapping at Adone", Proceedings of the XI-th International Conference on High Energy Accelerators, CERN - Geneva, July 1980, p.687 (1980).
- [19] D. A. Edwards, R. P. Johnson, F. Willeke: "Tests of Orbital Dynamics Using the Tevatron", Particle Accelerators, Vol. 19, No. 1-4, p.145 (1986).
- [20] P. L. Morton et al. : "Betatron Phase Advance Measurement at SPEAR", Proceedings of the 1987 IEEE Particle Accelerator Conference, Washington, March 1987, 87CH2387-9, p.1367 (1987).
- [21] J. Borer et al. : "Harmonic Analysis of Coherent Bunch Oscillations in LEP", Proceedings of the 3-rd European Particle Accelerator Conference, Berlin, March 1992 (1992).
- [22] S. Herb and F. Zimmermann: "Measurement by Tune Coupling of the Overlap of Colliding Bunches in HERA", Proceedings of the XV-th International Conference on High Energy Accelerators, Hamburg, July 1992, p.227 (1992).
- [23] A. Hofmann: "Diagnostics and Cures for Beam Instabilities", Proceedings of the XI-th International Conference on High Energy Accelerators, CERN - Geneva, July 1980, p.540 (1980).
- [24] J. M. Jowett et al. : "Beam Response Measurements at SPEAR", Proceedings of the 1-st European Particle Accelerator Conference, Rome, June 1988, p.726 (1988).
- [25] R. Boni et al. : "Investigations on Beam Longitudinal Transfer Function and Coupling Impedance in Adone", LNF-DM Note RM-23 (1981).
- [26] H. Hindi et al. : "Analysis of Bunch-by-Bunch DSP Based Longitudinal Feedback System: Trial at SPEAR", to be presented at the 1993 IEEE Particle Accelerator Conference, Washington, May 1993.